

## Article

# Field Test on Deformation Characteristics of Pile-Supported Reinforced Embankment in Soft Soil Foundation

Xin Wang<sup>1,2</sup>, Xizhao Wang<sup>3</sup>, Guangqing Yang<sup>1,4,\*</sup>, Changyu Pu<sup>5</sup> and Jinzhao Jin<sup>6</sup>

- <sup>1</sup> State Key Laboratory of Mechanical Behavior and System Safety of Traffic Engineering Structures, Shijiazhuang Tiedao University, Shijiazhuang 050043, China; wangx@stdu.edu.cn
- <sup>2</sup> School of Traffic and Transportation, Shijiazhuang Tiedao University, Shijiazhuang 050043, China
- <sup>3</sup> School of Civil Engineering, Hebei University of Science and Technology, Shijiazhuang 050018, China; wxizhao@hebest.edu.cn
- <sup>4</sup> School of Civil Engineering, Shijiazhuang Tiedao University, Shijiazhuang 050043, China
- <sup>5</sup> Hebei Provincial Communications Planning, Design and Research Institute Co., Ltd., Shijiazhuang 050011, China; puchangyu\_1980@163.com
- <sup>6</sup> Hebei Xiongan Rongwu Highway Co., Ltd., Baoding 071799, China; gtsyang@163.com
- \* Correspondence: yanggq@stdu.edu.cn

**Abstract:** In this work, the settlement deformation of the soft-soil subgrade and the deformation law of the geogrid were studied based on field tests carried out on the pile-supported reinforced embankment of the Rongwu Expressway in the Xiong'an New Area. The settlement and deformation law of the reinforcement area and the underlying layer of the pile-supported reinforced embankment, the settlement law of the transverse and longitudinal sections of the subgrade, and the deformation law of the bidirectional geogrid were analyzed. The results show that reducing the pile spacing and embankment height can effectively reduce the foundation settlement. The change in the pile spacing mainly affected the settlement in the reinforcement area, while the embankment height mainly affected the substratum settlement; the differential settlement in the subgrade cross-section was mainly caused by the settlement in the reinforcement area. The settlement at the center of the subgrade was obviously higher than that at the shoulder. In terms of the geogrid deformation law of the subgrade cross-section, the geogrid deformation at the center line of the subgrade was the largest. With the increase in the distance from the center line, the geogrid deformation gradually decreased. In terms of the deformation law of the biaxial geogrid, the tensile deformation of the geogrid in the center of two piles was greater than that in the center of four piles. The transverse tensile deformation of the geogrid was greater than the longitudinal tensile deformation. The tensile stress of the reinforced materials was calculated according to four specifications, and the applicability of various methods was evaluated.

**Keywords:** pile-supported reinforced embankment; foundation settlement; geogrid deformation; field test



**Citation:** Wang, X.; Wang, X.; Yang, G.; Pu, C.; Jin, J. Field Test on Deformation Characteristics of Pile-Supported Reinforced Embankment in Soft Soil Foundation. *Sustainability* **2022**, *14*, 7805. <https://doi.org/10.3390/su14137805>

Received: 23 May 2022

Accepted: 24 June 2022

Published: 27 June 2022

**Publisher's Note:** MDPI stays neutral with regard to jurisdictional claims in published maps and institutional affiliations.



**Copyright:** © 2022 by the authors. Licensee MDPI, Basel, Switzerland. This article is an open access article distributed under the terms and conditions of the Creative Commons Attribution (CC BY) license (<https://creativecommons.org/licenses/by/4.0/>).

## 1. Introduction

A pile-supported reinforced embankment is a complex geotechnical structure composed of a foundation, piles, pile caps, a reinforced cushion, and an embankment. A geogrid can promote the load transfer of stress from embankment filling to a pile cap, thereby reducing the uneven settlement in the surface of an embankment.

Research concerning reinforcement mechanisms has been carried out. Giroud [1,2] conducted a series of studies regarding the role of geogrids in reinforced embankments and proposed the tensioned membrane theory. Ghosh [3] proposed a mechanical model for a double-layer, geosynthetic-reinforced, pile-supported embankment. Zhao Minghua [4] comprehensively considered the interaction between each component of pile-supported reinforced embankments, and, as a result, used large deflection thin plate theory to analyze

the mechanical characteristics of the reinforced cushion. Abusharar [5] considered the role of shear stress on reinforcement, and then, combined with the relationship between the geometric size and the deformation of the reinforcement, the functional relationship between the tensile force and the deformation of the reinforcement was established. Finally, the deformation of the reinforcement was determined using the equilibrium equation. Zhuang Yan [6] assumed that the deformation shape of the reinforcement was similar to the elliptical parabolic surface and deduced the deformation expression of the reinforcement according to the three-dimensional deformation characteristics of the reinforcement. Xu Chao [7] studied the strain and stress characteristics of reinforcement in a three-dimensional state. In the calculation of the tensile stress of reinforcements, the Chinese Standard [8,9], British Standard [10], and Nordic Guidelines [11] all adopt the tensile membrane theory. This theory does not consider the bearing reaction of soil between the piles, and instead uses a simplified formula to calculate the tensile stress of reinforcements. The German Standard [12] assumes that the vertical load acting on the reinforcement has a triangular distribution, and that the maximum tensile stress of reinforcement occurs between two piles, which determines the maximum strain of the geogrid reinforcement. It can be seen that the deformation form and tension calculation of reinforcements have long been studied by scholars in various countries. However, due to the use of different theoretical bases and analysis methods, there are differences among the relevant standards in various countries. Therefore, in-depth understanding of the spatial distribution characteristics of the deformation of reinforced materials in pile-supported embankments is of great significance in the study of structural settlement control.

Research regarding the deformation characteristics of pile-supported reinforced embankments has also been carried out. Girout [13] and Zhu [14] studied the influence of geosynthetics on the deformation of pile-supported reinforced embankments through a model test. Cui [15] and Chen Yun-Min [16] explained the variation law of embankment settlements through a model test. They also analyzed the settlement distribution law and vertical stress distribution characteristics of pile-supported reinforced embankments. Reshma [17] studied the deformation characteristics of pile-supported reinforced embankments through a centrifugal model test. It was found that the deformation of an embankment with end-bearing piles was significantly smaller than that of an embankment that did not have pile-penetrating soft soil. Based on research surrounding field tests, Briancon [18] analyzed the load transfer mechanism and settlement deformation law of embankments. R. P. Chen [19] showed that substratum settlements account for a large proportion of the total settlement in an embankment, and the proportion of substratum settlement can be reduced by changing the pile length and, therefore, that the total settlement can be controlled. Cao [20] studied the reinforcement effect and the mechanism of pile-supported reinforcement technology in medium–low compressible soil and analyzed the deformation characteristics of foundation settlements and reinforced cushions. Zhang [21] studied the working behavior of pile-supported reinforced embankments in bridge head sections. The results showed that a pile-supported reinforced embankment can effectively control the levels of uneven settlement between a pavement and a bridge deck, improve the stability of an embankment, and solve the problem known as bridge head bumps. Although many scholars have studied the settlement deformation of pile-supported embankments, it shows that pile-supported reinforced embankment can effectively control subgrade settlement. However, there is no systematic study on the settlement law of the cross-section and longitudinal section of the pile-supported embankment.

Therefore, based on a field test carried out on the pile-supported reinforced embankment of the Rongwu Expressway in the Xiong'an New Area, this paper examines the settlement deformation of a soft-soil embankment and the deformation of a geogrid reinforcement during the construction period and 5 months after the completion of its construction. The reinforcement area, and the substratum settlements of horizontal and vertical sections of the pile-supported reinforced embankment, as well as the tensile deformation of the geogrid reinforcement at the center of two piles and four piles, were systematically ana-

lyzed. Then, according to the Chinese Standard, British Standard, German Standard, and Nordic Guidelines, the evaluation index of the geogrid was calculated, and the calculation results for each standard were compared and analyzed.

## 2. Engineering Situations and Test Scheme

### 2.1. Engineering Situations

As shown in Figure 1, the test section was located in the bridge–subgrade transition section of the Rongwu Expressway in the Xiong’an New Area. The test section was located in the alluvial plain area with relatively flat terrain, and the groundwater depth was 9.5~10.5 m. The thickness and distribution of the foundation soil layer are shown in Figure 2. The main physical and mechanical parameters of the foundation soil layer were obtained through geological survey, as shown in Table 1.



Figure 1. Geographical location of the test section.

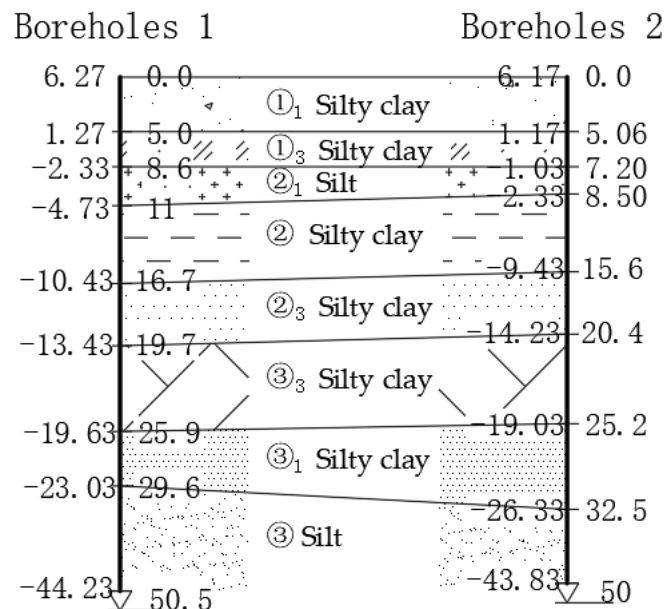


Figure 2. Distribution of the foundation soil layers.

**Table 1.** Engineering properties of the soil layer in the test section.

No.	Soil Layer	Main Physics Targets					Main Mechanical Indexes			
		Water Content $\omega$ [%]	Unit Weight $\gamma$ [kN/m <sup>3</sup> ]	Void Ratio $e$	Liquid Limit $\omega_L$ [%]	Plastic Limit $\omega_p$ [%]	Coefficient of Compressibility $a_{1-2}$ [Mpa <sup>-1</sup> ]	Modulus of Compression $E_{s1-2}$ [MPa]	Force of Cohesion $c$ [kPa]	Angle of Internal Friction [°]
① <sub>1</sub>	Silty clay	24.9	19.2	0.778	32.2	18.8	0.32	6.3	24.5	13.8
① <sub>3</sub>	Silty clay	33.4	18.2	1.007	37.9	21.4	0.45	4.5	24.8	11.4
② <sub>1</sub>	Silt	21.2	19.1	0.718	26.2	17.4	0.23	8.7	11.5	20.8
②	Silty clay	24.2	19.6	0.737	31.2	18.7	0.31	5.9	24.7	12.9
② <sub>3</sub>	Silty clay	35.4	18.4	1.018	39.4	22.5	0.50	4.2	22.6	41.1
③ <sub>3</sub>	Silty clay	33.5	18.9	0.932	37.2	21.5	0.47	4.1	18.5	15.5
③ <sub>1</sub>	Silty clay	24.1	20.0	0.691	30.5	18.0	0.33	5.8	26.7	15.5
③	Silt	19.8	20.4	0.588	25.8	16.6	0.23	8.8	12.8	21.3

## 2.2. Field Test Design

Soft-soil foundations are treated with prestressed pipe piles; here, the strength of the prestressed pipe pile concrete was C60. The prestressed pipe piles were distributed squarely, and the pile length was 14m. The pile spacing was 2 m, 2.2 m, and 2.5 m, respectively, from the bridge abutment to the embankment, and the pile top was a 1.0 m × 1.0 m × 0.3 m C30-reinforced concrete pile cap. The thickness of the cushion was 0.3 m, which adopted two forms, as follows: a gravel cushion and a geogrid-reinforced gravel cushion. The main technical parameters of the test section are shown in Table 2.

**Table 2.** Technical indexes of subgrade cross-section in test section.

No.	Foundation Treatment Methods	Cushion Thickness [m]	Embankment Height [m]	Pile Length [m]	Pile Diameter [m]	Pile Spacing [m]
Section I	Prestressed Pipe Pile + Gravel Cushion	0.3	7.2	14	0.4	2.0
Section II	Prestressed Pipe Pile + Gravel Cushion	0.3	7.2	14	0.4	2.5
Section III	Prestressed Pipe Pile + Geogrid + Gravel Cushion	0.3	5.3	14	0.4	2.0
Section IV	Prestressed Pipe Pile + Geogrid + Gravel Cushion	0.3	5.1	14	0.4	2.2
Section V	Prestressed Pipe Pile + Gravel Cushion	0.3	5.0	14	0.4	2.5

Sections I and II were located in the road–bridge transition section of the Tulou Separated Interchange; sections III, IV, and V were located in the road–bridge transition section of the Tulou Middle Bridge. In the test, a flexible displacement meter was used to monitor the geogrid deformation of the reinforced cushion, and a single-point settlement gauge was used to monitor the foundation settlement. The layouts of the monitoring instruments are shown in Figure 3.

In sections III and IV, flexible displacement gauges were embedded in the horizontal and vertical directions on the geogrid at the subgrade center, 10m to the right of the centerline, and on the road shoulder. The flexible displacement gauges were located between the pile caps, and six flexible displacement gauges were embedded in each test section. Flexible displacement gauges No. 1, 2, 3, and 6 were used to test the tensile deformation of the geogrid at the center of two piles and at the center of four piles in the direction of the embankment cross-section. Flexible displacement gauges No. 4 and 5 were used to test the tensile deformation of the geogrid at the center of the two piles and at the center of the four piles in the direction of the longitudinal line. In sections I, II, III, and V, a single-point settlement gauge was set at the cushion bottom at the subgrade center and shoulder, and four single-point settlement gauges were set for each section. The depths of the measuring rods of the single-point settlement gauges were 14 m and 30 m, respectively, which were used to test the settlement in the reinforcement area and in the underlying layer of the soft-soil foundation.

Field test data acquisition met the following requirements:

- (1) Before embankment filling, all of the buried sensors were retested, and the measured value was the initial reading;
- (2) During the embankment filling, the data from all of the monitoring points were collected once a day. The daily data collection time was fixed to ensure the same time interval was used;
- (3) After the embankment filling was completed to the end of the observation period, measurement was carried out every 3 days;
- (4) The monitoring data were sorted in a timely manner, and retests were carried out if the data change was large.

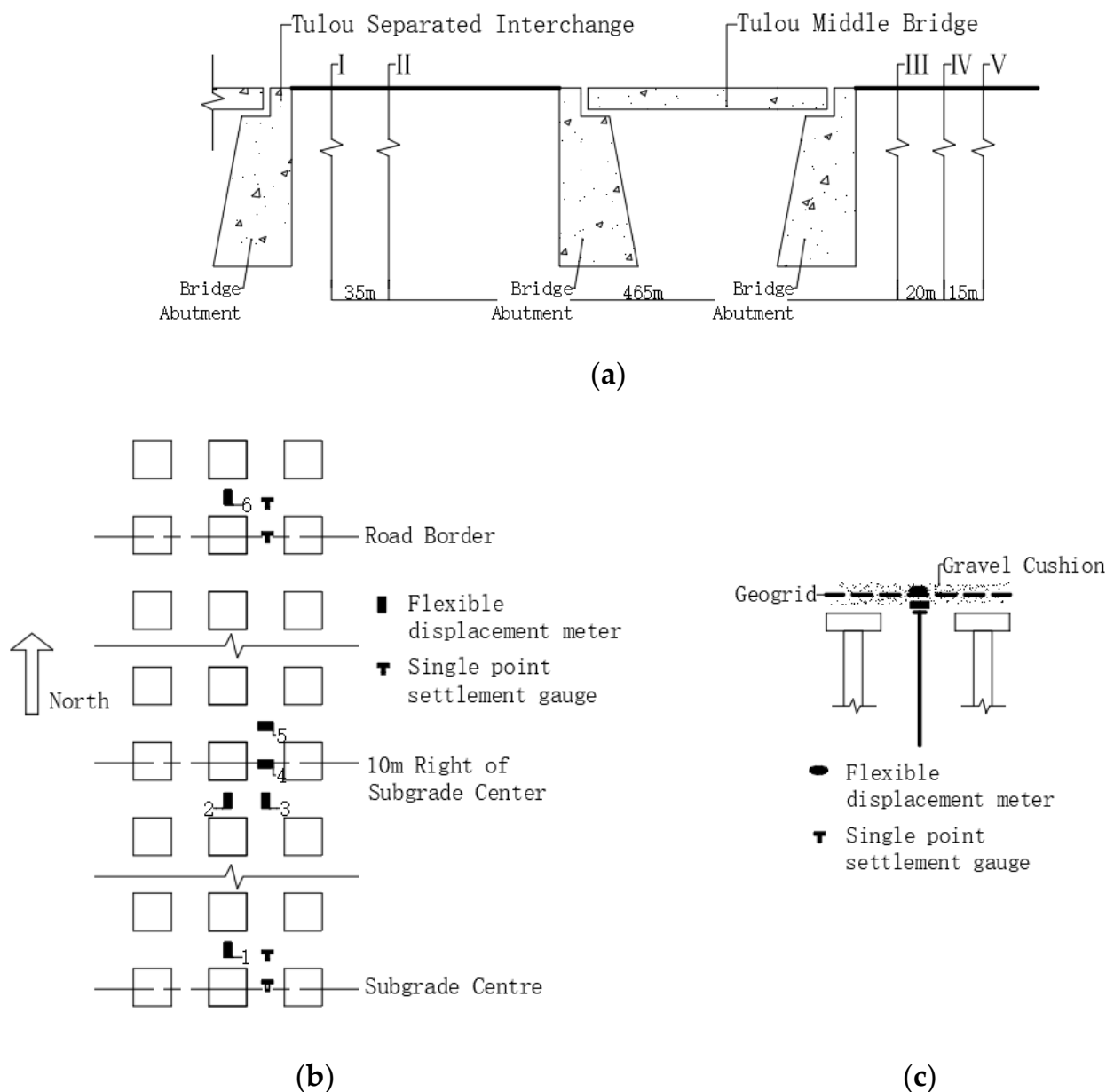


**Figure 3.** Schematic diagram of the monitoring element embedding; (a) Distribution of test section; (b) Distribution of monitoring elements on cross-section; (c) Distribution of monitoring elements on vertical section.

### 3. Analysis of Test Results

The field test observation began from the embankment filling and lasted until 5 months after its completion. The construction period in sections I and II was 0–60 days, and the construction period of sections III, IV, and V was 0–35 days.

#### 3.1. Foundation Settlement

##### 3.1.1. Influence of Pile Spacing on Foundation Settlement

As shown in Figure 4, it can be seen from the settlement curves in sections I and II that the settlement in the reinforcement area and the underlying layer of each test section increased gradually during the embankment construction, and that the settlement growth rate of the underlying layer was significantly higher than that of the reinforcement area. During the post-construction observation period, the settlement increase in the reinforcement area was small, gradually becoming stable, and the substratum settlement

increased significantly, but the growth rate was significantly smaller than that during the construction period. It can be seen that the settlement in the reinforcement area was greatly affected by construction, and that the settlement increased significantly with the increase in upper load during embankment filling. In addition to the influence of the embankment load, the substratum settlement was also affected by the consolidation of foundation soil. The pore water gradually discharged under pressure, the void ratio decreased, and the settlement increased. In Table 3, it can be seen that the settlement increases in the reinforcement areas of Sections I and II were 24% and 19%, respectively, and that the increases in the substratum settlement were 46% and 57%, respectively. This indicates that the substratum settlement increased significantly during the post-construction observation period, while the settlement in the reinforcement area was basically completed during the construction period. In other words, post-construction subsidence was mainly caused by the substratum settlement.

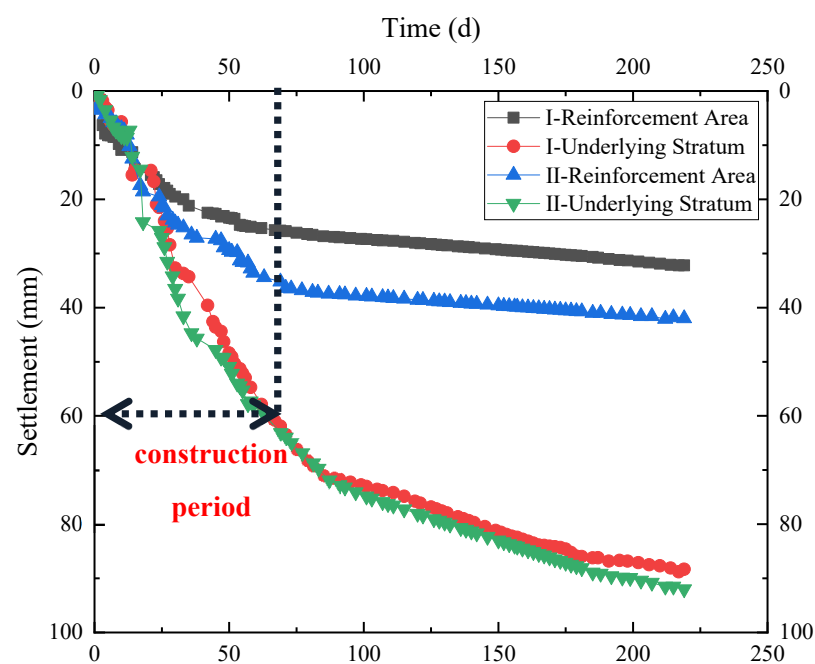


Figure 4. Foundation settlement deformation curve of sections I and II.

Table 3. Settlement values of sections I and II at each observation stage.

	Section I		Section II		Settlement Difference of Sections I and II	
	End of Construction	End of Observation Period	End of Construction	End of Observation Period	End of Construction	End of Observation Period
Reinforcement Area Settlement [mm]	25	31	36	43	−11	−12
Substratum Settlement [mm]	61	89	58	91	3	−2
Total Settlement [mm]	86	120	94	134		

As shown in Table 3, at the end of the observation period, the difference in sedimentation in the reinforcement area of section I and II was 12 mm, and the difference in sedimentation in the underlying layer was 2 mm. This shows that pile spacing had a great influence on the settlement in the reinforcement area, and the settlement in the reinforcement area increased with the increase in pile spacing, while the substratum settlement did not change significantly. The main reason for this is that the bearing capacity of a single pile was weakened with the increase in pile spacing, and the soil between the piles

bore more of a load, so the settlement in the reinforcement area increased. The underlying layer mainly bore the load transmitted by the pile and the soil between the piles. As the embankment heights in sections I and II were the same, the additional load generated by embankment filling was the same. Therefore, the total load transferred through piles and soil between the piles was the same, meaning that the substratum settlement was less affected by pile spacing.

As shown in Figure 5, it can be seen that the substratum settlement accounted for a larger proportion of the total settlement in different observation periods. Compared with Table 3, the settlement increase in the reinforcement area of sections I and II was 24% and 19%, respectively. Compared with section II, the settlement in the reinforcement area of section I increased greatly. This shows that the settlement in section I increased greatly during the post-construction observation period; that is, the settlement in the reinforcement area increased slightly during the construction stage. The main reason for this is that smaller pile spacing was adopted in section I, and a pile could share more additional load. Therefore, the settlement in the reinforcement area could be effectively controlled during the construction process. However, during the post-construction observation period, the settlement in the reinforcement area increased gradually with the consolidation of the foundation.

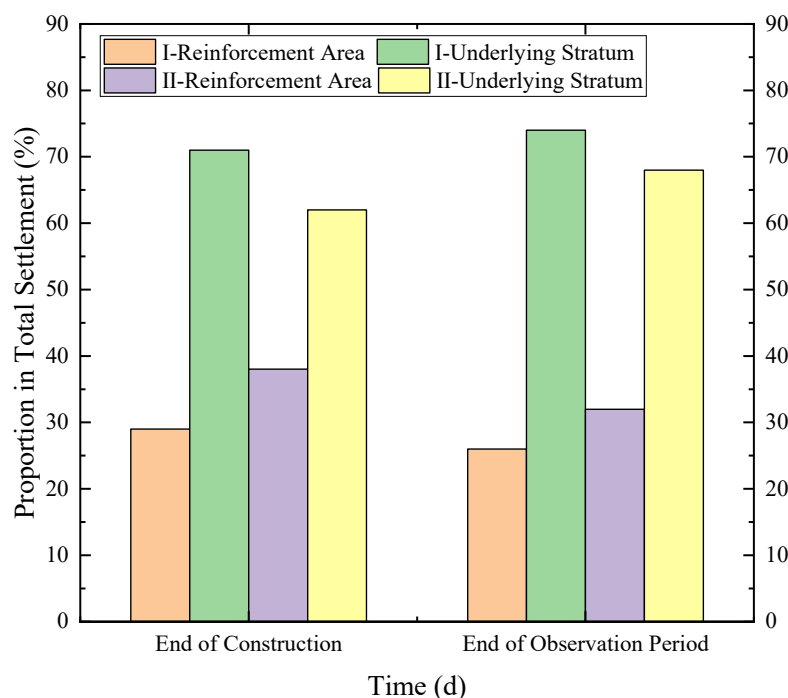


**Figure 5.** Settlement proportion of the reinforcement area and underlying layer in sections I and II.

Therefore, from a macro point of view, smaller pile spacing could effectively reduce the total settlement in the foundation. From the perspective of settlement position, the settlement in the reinforcement area was mainly reduced through the adoption of smaller pile spacing. From the perspective of settlement growth, smaller pile spacing could effectively reduce the settlement during the construction stage of the reinforcement area.

### 3.1.2. Influence of Embankment Height on Settlement

As shown in Figure 6, the subsidence laws in sections II and V were basically the same. During the construction stage, the settlement in the reinforcement area and the underlying layer at each measuring point gradually increased, and the substratum settlement increased greatly. During the post-construction observation period, the increase in settlement in the reinforcement area decreased and gradually became stable. The substratum settlement

increased significantly, but the growth rate was significantly slower than during the construction period. In Table 4, it can be seen that the settlement increases in reinforcement areas in sections II and V were 19% and 35%, respectively, and that the increase in substratum settlement was 57% and 51%, respectively. This indicates that the substratum settlement increased significantly during the post-construction observation period; that is, post-construction settlement was mainly caused by substratum settlement.

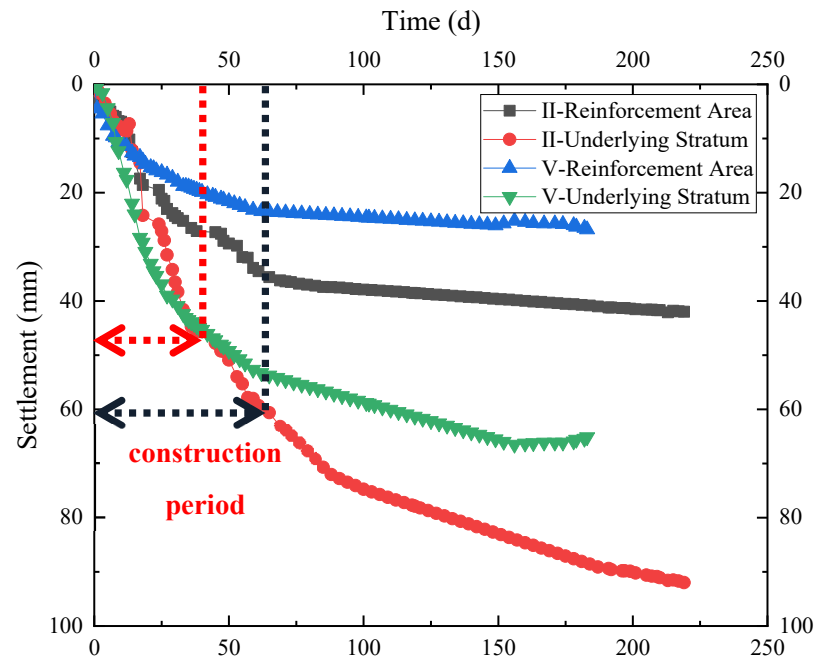


Figure 6. Foundation settlement deformation curve of sections II and V.

Table 4. Settlement values of sections II and V at each observation stage.

	Section II		Section V		Settlement Difference of Sections II and V	
	End of Construction	End of Observation Period	End of Construction	End of Observation Period	End of Construction	End of Observation Period
Reinforcement Area Settlement [mm]	36	43	20	27	16	16
Substratum Settlement [mm]	58	91	43	65	15	26
Total Settlement [mm]	94	134	63	92		

As shown in Table 4, at the end of the observation period, the sedimentation difference in the reinforcement areas of sections II and V was 16 mm, and the settlement difference in the underlying layer was 26 mm. This shows that with the increase in embankment height, the settlement in the reinforcement area and underlying layer increased, but the substratum settlement increased more. The main reason for this was that the underlying layer supports more the whole load from the pile and the soil between piles, so it was greatly affected by the height of the embankment.

As shown in Figure 7, by the end of the observation period, the substratum settlement in sections II and V accounted for 68% and 71% of the total settlement, respectively. This shows that the substratum settlement accounted for the largest proportion of the total settlement, and the foundation settlement was mainly caused by the substratum settlement. In Table 4, it can be seen that the settlement increases in the reinforced areas of sections II and V were 19% and 35%, respectively. Compared with section II, the settlement in

the reinforcement area of section V increased greatly. This shows that the settlement in section V increased greatly during the post-construction observation period; that is, the settlement in the reinforcement area of section V increased slightly during the construction stage. The main reason for this was that the embankment height of section V was low, the embankment load was small, and the stress acting on the soil between piles was small after the distribution of the soil arching effect. Therefore, the settlement growth range in the reinforcement area was small during the construction process.

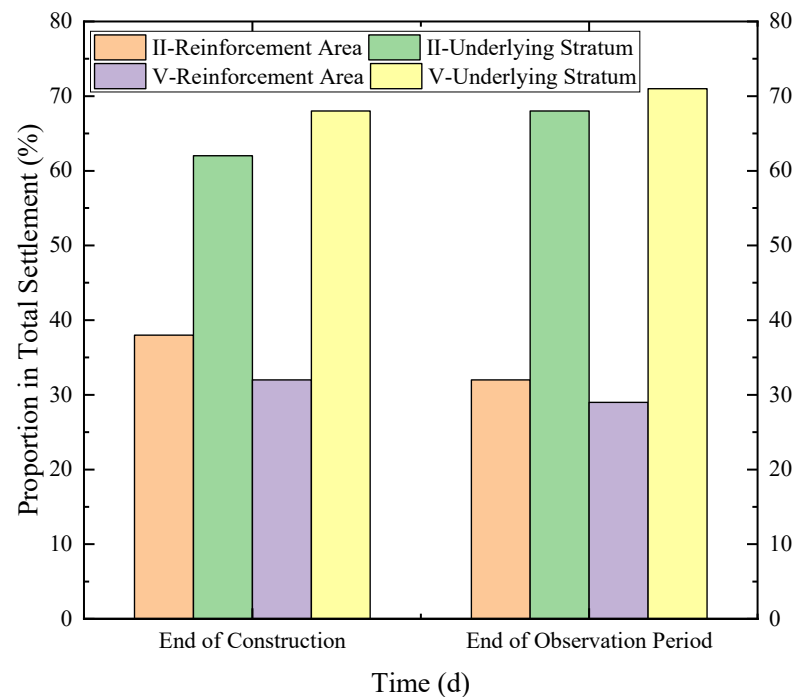


**Figure 7.** Settlement proportion of the reinforcement area and underlying layer in sections II and V.

Therefore, from a macro perspective, a smaller embankment height could effectively reduce the total settlement in the foundation. From the settlement perspective, the substratum settlement was mainly reduced by using smaller embankment heights. From the perspective of settlement growth, smaller embankment heights can effectively reduce the settlement during the construction stage of the reinforcement area.

As shown in Tables 3 and 4, by the end of the observation period, the total foundation settlement in sections I, II, and V was 120 mm, 134 mm, and 92 mm, respectively. Compared with section II, the total foundation settlement in section I decreased by 10.4%, and that of section II decreased by 31.3%. It can be seen that reducing pile spacing and embankment height can reduce the total foundation settlement, but the embankment height has a greater impact on the settlement in the foundation.

### 3.2. Settlement Analysis of Wide Subgrade Section

#### 3.2.1. Settlement Deformation Law of Subgrade Cross-Section

As shown in Figure 8, during embankment construction, the settlement in the reinforcement area and the underlying layer gradually increased, and the growth rate of the substratum settlement was significantly higher than that of the reinforcement area. During the post-construction observation period, the substratum settlement increased significantly, but the growth rate was less than that during the construction period, and the settlement values of each measuring point had little difference between each other. The increase in the settlement in the reinforcement area decreased and tended to be stable, and the settlement values in the reinforcement area of each measuring point were significantly different. The differential settlement in the subgrade cross-section was mainly caused by the settlement in

the reinforcement area. By the end of the observation period, the settlement at the subgrade center and shoulder of section III was 91 mm and 83 mm, respectively. This indicates that the settlement at the center of subgrade was greater than that at the shoulder.

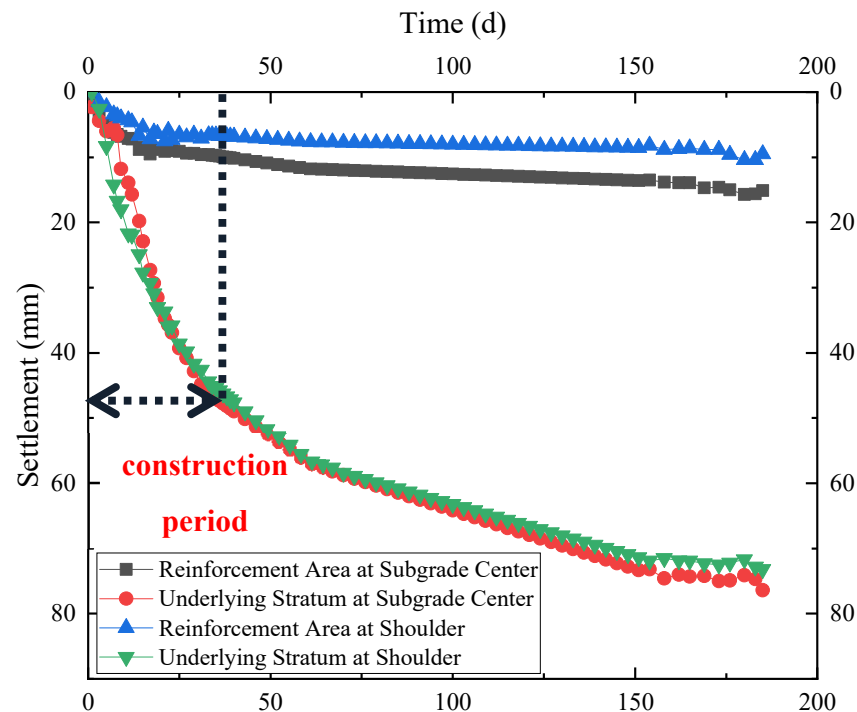


**Figure 8.** Settlement deformation of subgrade cross-section of section III.

The settlement law in each test section was similar, and the substratum settlement accounted for a larger proportion of the total settlement. The settlement in the reinforcement area and the underlying layer at the center of the embankment was greater than that at the corresponding position of the shoulder. As shown in Table 5, by the end of the observation period, the settlement difference in the subgrade cross-section of sections I and II was 12 mm and 17 mm, respectively. This shows that the uneven settlement in the subgrade cross-section increased with the increase in pile spacing. The settlement difference in the reinforced area of sections I and II was 8 mm and 13 mm, respectively, while the settlement difference in the underlying layer was the same, which was 4 mm. This shows that the change in pile spacing had little effect on the settlement difference in the underlying layer.

**Table 5.** Settlement value of the subgrade cross-section of section I and II.

Test Section	Test Position	Reinforcement Area Settlement [mm]	Substratum Settlement [mm]	Total Settlement [mm]	Proportion of Settlement Difference in Reinforcement Area [%]
Section I	Subgrade Centre	31	89	120	
	Road Border Settlement	23	85	108	
	Difference of Cross-section	8	4	12	66.6
Section II	Subgrade Centre	43	91	134	
	Road Border Settlement	30	87	117	
	Difference of Cross-section	13	4	17	76.5

Therefore, from a macro point of view, as pile spacing increased, the differential settlement in the subgrade cross-section increased. From the perspective of settlement position, the settlement in the reinforcement area of the subgrade cross-section increased with the increase in pile spacing.

As shown in Table 6, by the end of the observation period, the settlement difference in the subgrade cross-section of sections II and V was 17 mm and 9 mm, respectively. This shows that the uneven settlement in the subgrade cross-section decreased with the decrease in embankment height. By the end of the observation period, the settlement difference in the reinforced area of sections II and V was 13 mm and 9 mm, respectively, with a decrease of 30.8%. The settlement difference in the underlying layer of sections II and V was 4 mm and 0 mm, respectively, with a decrease of 100%. The change in embankment height had an impact on the settlement difference in the reinforced area and the underlying layer, but it had a greater impact on the settlement in the underlying layer.

**Table 6.** Settlement value of subgrade cross-section of section II and V.

Test Section	Test Position	Reinforcement Area Settlement [mm]	Substratum Settlement [mm]	Total Settlement [mm]	Proportion of Settlement Difference in Reinforcement Area [%]
Section II	Subgrade Centre	43	91	134	
	Road Border	30	87	117	
	Settlement Difference of Cross-section	13	4	17	76.5
Section V	Subgrade Centre	27	65	92	
	Road Border	18	65	83	
	Settlement Difference of Cross-section	9	0	9	100

Therefore, from a macro point of view, the differential settlement in the subgrade cross-section decreased with the decrease in embankment height. In terms of settlement position, reducing the height of the embankment reduced the settlement in the reinforcement area and the substratum on the subgrade cross-section. Among these, the substratum settlement decreased the most.

The main reason for the phenomenon discussed above is that piles in the test section were friction piles, which had not penetrated the soft-soil layer. After embankment filling, the foundation needed a period of time to be stable, and the settlement in the underlying layer was relatively large. Therefore, the substratum settlement accounted for a larger proportion of the total settlement. The soil properties of the underlying layer in the same test section were basically the same. Therefore, under the action of the upper load, there was little difference in the substratum settlement in the subgrade cross-section. As the road shoulder was the free surface of the side slope, in addition to the vertical pressure of the embankment filling, it was also subjected to the thrust generated by the lateral slip of the side slope, and the stress state is different from that at the center of the subgrade. Therefore, the settlement law at the shoulder and the center of the subgrade was different. Therefore, the settlement in the reinforcement area of the subgrade cross-section displayed a certain difference.

### 3.2.2. Settlement Deformation Law of Subgrade Longitudinal Section

Due to the large differences in the stiffness of the abutment, embankment filling, and subgrade materials, different subgrade designs were adopted for sections III and V to reduce the bump at the bridge head. Section III was close to the bridge head. In order to effectively control the settlement, smaller pile spacings and reinforced cushions were used

in section III. As the distance from the bridge head increased, the pile spacing gradually increased to achieve a smooth transition in the bridge head section.

As shown in Table 7, due to the different embankment designs in sections III and V, the settlement in the reinforcement area and the underlying layer of each section was different, but the total settlement in the subgrade was basically the same. The main reason for this was that the smaller pile spacing in section III was conducive to the exertion of the soil arching effect. Additionally, section III laid a reinforced cushion. The friction and occlusion between soil particles and the geogrid interface were strong, and part of the stress in the soil was diffused and transferred. Therefore, the shear stress in the soil decreased, and the bearing capacity and deformation resistance of the soil were significantly improved, so that the differential settlement could be controlled more effectively. To effectively reduce the differential settlement in the road–bridge transition section, in addition to the reasonable control of pile spacing, a reinforced cushion can be used to enhance the load transfer efficiency.

**Table 7.** Embankment design and settlement value of sections III and V.

Test Section	Distance from Bridge Head [m]	Pile Spacing [m]	Embankment Height [m]	Cushion Form	Reinforcement Area Settlement [mm]	Substratum Settlement [mm]	Total Settlement [mm]	Proportion of Substratum Settlement [%]
Section III	14	2	5.3	Reinforced Cushion	15	76	91	84
Section V	54	2.5	5.0	Gravel Cushion	27	65	92	71

### 3.3. Geogrid Deformation Analysis of Wide Subgrade Section

#### 3.3.1. Geogrid Deformation Law of Subgrade Cross-Section

Figure 9 displays the tensile strain curve of the geogrid in section III. The tensile strain of the geogrid at the center of the subgrade was larger than that at the shoulder. During the construction process, the geogrid strain at each observation point increased rapidly with the increase in the filling height, and the growth rate of the geogrid strain at the center of the embankment was the largest. During the post-construction observation period, the geogrid strain at each observation point increased slightly and gradually stabilized. By the end of the observation period, the geogrid strains of the subgrade center, the right side of the centerline, and the shoulder were 0.26%, 0.24%, and 0.08%, respectively. This shows that the geogrid deformation at the subgrade centerline was the largest. With the increase in the distance from the subgrade centerline, the geogrid deformation decreased gradually, and the geogrid deformation at the shoulder decreased significantly. In Figure 8, it can be seen that the deformation characteristics of the geogrid were similar to the settlement law, indicating that the deformation of the geogrid was related to the foundation settlement.

#### 3.3.2. Analysis of Transverse and Longitudinal Tensile Deformation of Geogrid

As shown in Figure 10, during the construction process, the geogrid strain of each observation point increased rapidly with the increase in the filling height. During the post-construction observation period, the grid deformation at each observation point was basically stable. It can be seen from the geogrid deformation law that the geogrid strain in the center of two piles was greater than that in the center of four piles, and that the transverse strain was greater than the longitudinal strain. Additionally, the grid strain at the corresponding position of section IV was greater than that of section III.

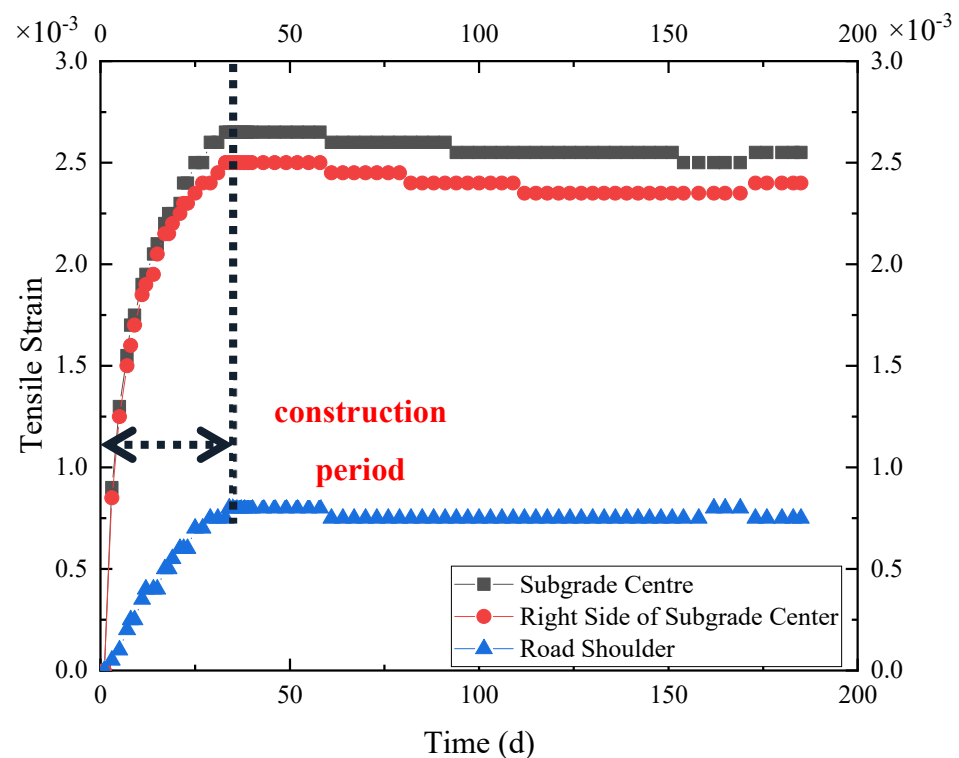
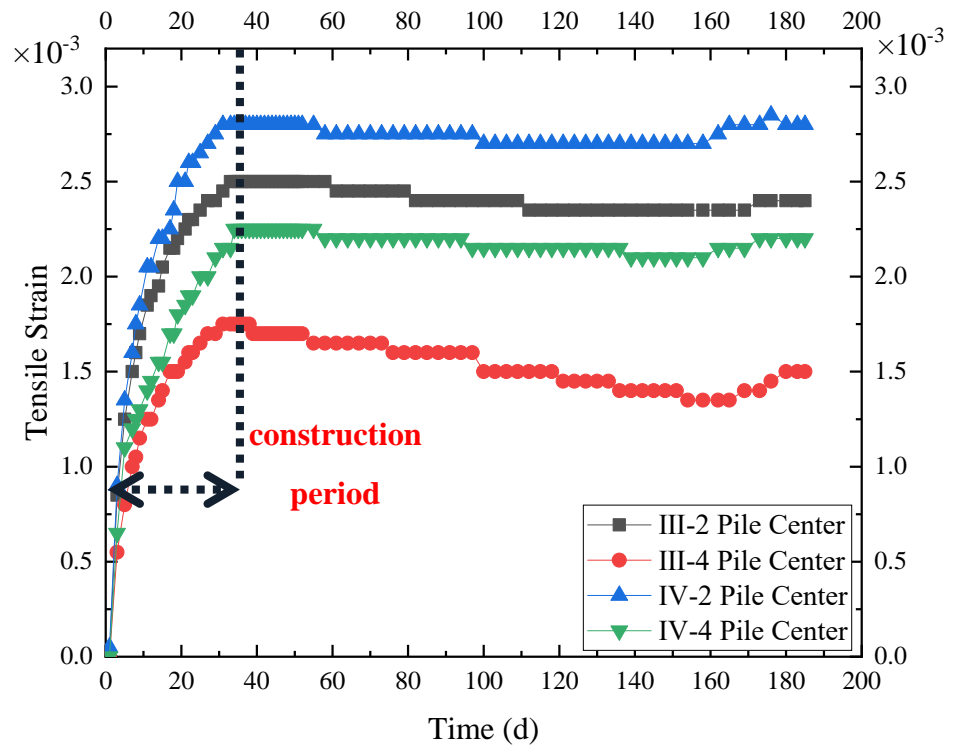


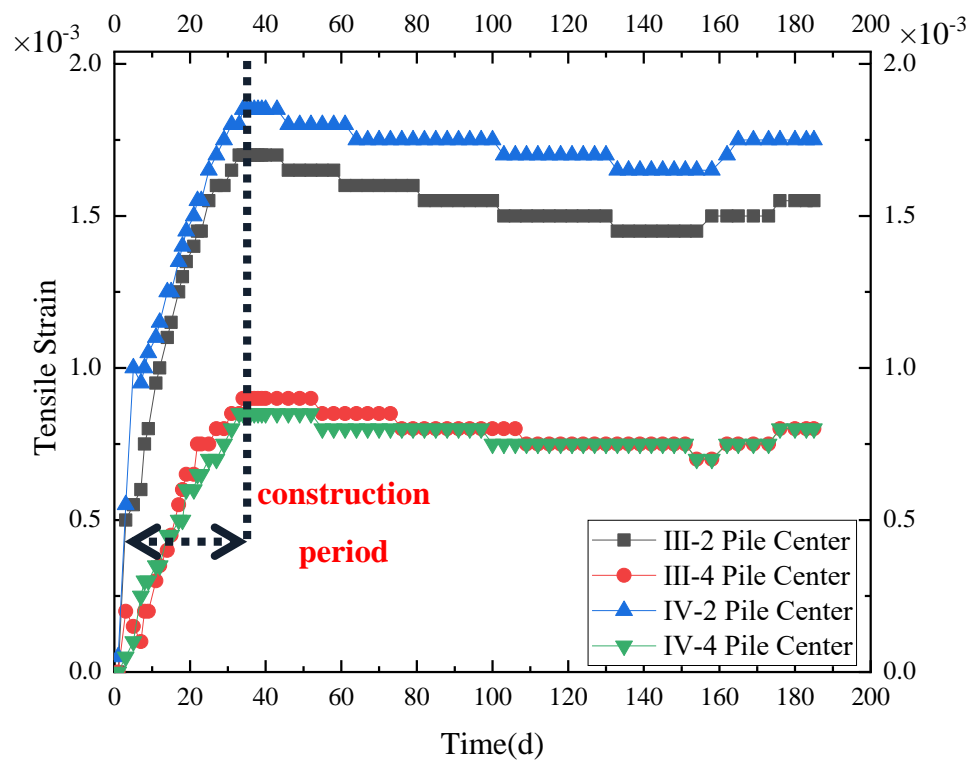
**Figure 9.** Tensile strain of geogrid in section III.

The main reason for this was that the friction between the pile cap and the reinforcement was large, and the displacement of the reinforcement was limited. The deformation space in the reinforcement between two piles was smaller than that between four piles, so the geogrid strain at the center of two piles was larger after the reinforcement was subjected to a vertical load. Secondly, the reinforcement at the center of the four piles displayed a certain deformation, indicating that this part of the reinforcement bore and transferred load. Therefore, it is suggested that the three-dimensional deformation of reinforced materials should be considered in the calculation of the tensile membrane effect. The stress on the cross-section of the embankment mainly came from the following two aspects: the first was the vertical load generated by the gravity of the embankment, and the second was the thrust generated by the lateral slip at the slope. The transverse grid played a role in limiting the settlement and horizontal deformation of the embankment, so the transverse tensile strain of the geogrid was larger. Compared with section III, the spacing between the piles in section IV was larger, which was not conducive to the exertion of the soil arching effect. Therefore, the soil between the piles bore more upper loads, and the geogrid deformation was more obvious. By the end of the observation period, the grid strain of each measuring point was less than 0.3%, so in order to give full play to the coordinated deformation of the geogrid, the use of a low-strength geogrid is recommended.

In summary, in terms of the geogrid deformation law on the subgrade cross-section, from the center of the subgrade to the shoulder, the deformation of the geogrid decreased gradually and decreased significantly in the shoulder. In the analysis of the deformation law of the biaxial geogrid, the grid strain at the center of two piles was shown to be larger than that at the center of four piles, and the transverse strain was larger than the longitudinal strain.



Transverse tension deformation of geogrid



Longitudinal tension deformation of geogrid

Figure 10. Tensile strain of geogrid in sections III and IV.

### 3.3.3. Comparison between Design Value and Measured Value

The soil arching effect in the embankment and the membrane effect of the geogrid in a reinforced cushion are the core components of the load transfer mechanism in pile-supported reinforced embankments. The stress and strain of the geogrids were calculated according to the Chinese Standard, British Standard, German Standard, and Nordic Guidelines, and the applicability of various methods was evaluated by comparing the measured results.

As shown in Table 8, after the completion of embankment filling, the measured strain of reinforcement in each test section was far lower than the design value of each specification. The strain values of reinforcement in the design codes of various countries can be compared. Indeed, GB/T 50783-2012 [11] stipulates that the strain rate corresponding to the tensile strength of geogrid design is 4–6%, which is significantly higher than other specifications, indicating that the Chinese Standard is relatively conservative. The transverse tensile strain of the geogrid in the center of sections III and IV was 0.26% and 0.37%, respectively, indicating that the geogrid deformation increased with the increase in pile spacing. However, the maximum long-term allowable strain of the reinforcement was directly set in the Chinese Standard and the British Standard without considering the influence of pile spacing, which deviated greatly from the actual situation.

**Table 8.** Comparison of measured and calculated values of grid deformation.

	Geogrid Strain [%]		Tensile Stress of Geogrid [kN/m]	
	Section III	Section IV	Section III	Section IV
measured value	0.26	0.37	7.8	11.1
Chinese Standard		4–6	45.7–53.4	73.2–85.6
German Standard	2	2.5	60	75
Nordic Guidelines	0.7–3	0.6–2.6	31.7–63.6	48.5–96.2
BS 8006-1-1		3	39.5	71.9
BS 8006-1-2		3	23	49.3

The measured tensile stress of the geogrid was far lower than the design value of each specification, and the calculation results for each specification were also quite different. The main reason for this was that the current theoretical calculation adopted simplified analysis methods. Firstly, it was assumed that part of the embankment load was directly transmitted to the pile cap through the soil arching effect and borne by the pile, while the remaining loads were all applied to the reinforcement. Then, the force analysis and deformation calculation were carried out according to the assumed deformation shape of the reinforcement. Due to different assumptions regarding the soil arch shape and the deformation mode of the reinforced material, the theoretical values obtained based on different calculation models were quite different. This situation led to great differences in the design criteria and analysis methods for a pile-supported reinforced embankment.

The selection of a calculation model of the soil arching effect was carried out. The first algorithm proposed by the British Standard (BS 8006-1-1) uses the Marston theory [22] to estimate the earth pressure at the top of the pile, considering that the soil arch in the embankment is the vertical shear plane. The second algorithm from the British Standard (BS 8006-1-2) is based on the Hewlett and Randolph [23] soil arch model, which is the calculation formula of the load-sharing ratio obtained in the limit state. However, in fact, neither the soil element at the top of the pile cap nor the soil element at the top of the soil arch enters the limit state. Therefore, Chen [24] introduced parameter  $\alpha$  to determine whether soil enters the plastic state, and modified the Hewlett and Randolph soil arch model, which was adopted by JTG/Td31-02-2013. The Nordic Guidelines adopt the wedge soil arch model proposed by Carlsson, which considers the load acting on the soil between piles to always be equal to the weight of the wedge and does not consider it to be affected by the height of the embankment. The EBGeo 2010 adopts the multi-arch model proposed

by Zeaske and Kempfert [25] to consider the influence of embankment load and external load on the reinforcement between piles.

For the calculation of the tensile stress of a reinforcement, the tensile membrane theory is adopted in the Chinese Standard, British Standard, and Nordic Guidelines, without considering the supporting reaction of soil between piles. The simplified formula is used to calculate the tensile stress of a reinforcement, which is too conservative. Most standards adopt the tensile membrane theory in the calculation of tensile stress. However, due to the use of different calculation models for the determination of the soil arching effect, the calculation results regarding reinforcement force are quite different. The German Standard considers the supporting force of soil between piles and the tensile stiffness of reinforced materials. In the calculation, the average compressive stress on the cushion is converted to the triangular-distributed load on the strip between piles, and the maximum stress on the reinforcement is assumed to occur in the width range of the pile cap. According to the vertical force balance of the reinforcement in the width range, the average strain of the reinforcement can be determined. Although the German Standard does not need to assume the deformation curve of the reinforcement, which is a relatively more reasonable method of describing the deformation of the reinforcement, it determines the average strain of the reinforcement and cannot reflect the stress of the reinforcement along the length direction.

In summary, in the calculation of reinforcement tension, the design value of standards in various countries is much larger than the measured value. The reinforcement strain in standards is mostly taken from empirical values, and the designs are relatively conservative. On a theoretical basis, the German Standard is more comprehensive.

#### 4. Conclusions

Based on a field test carried out on a pile-supported reinforced embankment of the Rongwu Expressway in the Xiong'an New Area, we studied the settlement deformation of soft-soil subgrade and the deformation law of geogrids. The influencing factors of settlement in reinforcement areas and underlying layers, settlement in transverse and longitudinal sections of the subgrade, and the transverse and longitudinal tensile deformation of geogrids were analyzed. The results show the following:

- (1) Reducing pile spacing and embankment height can effectively reduce the total settlement in subgrades and uneven settlement in subgrade cross-sections. A change in pile spacing mainly affects the settlement in reinforcement areas, while the embankment height mainly affects the substratum subsidence.
- (2) Differential settlement in subgrade cross-sections is mainly caused by settlement in reinforcement areas. The settlement at the center of a subgrade is significantly higher than that at the shoulder.
- (3) Reinforced material has a certain effect on the homogenization of embankment settlements. In order to effectively reduce the differential settlement in the road-bridge transition section, a reinforced cushion can also be used to enhance the load transfer efficiency.
- (4) In terms of the geogrid deformation law of subgrade cross-sections, the geogrid deformation at the center line of a subgrade is the largest. With the increase in distance from the center line, the geogrid deformation decreases gradually. With regard to the deformation law of biaxial geogrids, the tensile deformation of the geogrid in the center of two piles is greater than that in the center of four piles. The transverse tensile deformation of a geogrid is greater than the longitudinal tensile deformation. With the increase in pile spacing, the geogrid deformation is more obvious.
- (5) In the field test, the measured values of reinforcement strain and tensile stress were shown to be far lower than the design values of each specification. Due to the different theoretical bases and analysis methods, there were differences between the national standards. On a theoretical basis, the German Standard is more comprehensive.

In summary, in this paper, the deformation characteristics of pile-supported reinforced embankments were analyzed using field tests. The test results show that the geogrid at the

center of four piles underwent a certain deformation, but most calculation methods only consider geogrid deformation between two piles, ignoring the contribution of reinforcement between four piles to load transfer. The structure of a pile-supported embankment is complex, and different calculation methods are used. Therefore, in engineering design, various methods should be adopted for comprehensive analysis combined with engineering characteristics.

**Author Contributions:** Writing—original draft preparation, X.W. (Xin Wang); writing—review & editing, X.W. (Xizhao Wang); funding acquisition, G.Y.; validation, C.P. and J.J. All authors have read and agreed to the published version of the manuscript.

**Funding:** This research was supported by the National Natural Science Foundation of China (Grant No.52079078); the Key R&D Projects in Hebei Province (Grant No.20375504D); the Hebei Provincial Department of Transportation Science and Technology Project (Grant No.RW-202014); and the Innovation Funding Project for Postgraduates in Hebei Province (Grant No. CXZZBS2022121).

**Data Availability Statement:** The data used to support the findings of this study are available from the corresponding author upon request.

**Conflicts of Interest:** The authors declare no conflict of interest.

## References

- Giroud, J.P.; Han, J. Design method for geogrid-reinforced unpaved roads (part I): Theoretical development. *J. Geotech. Geoenviron. Eng.* **2004**, *130*, 776–786. [[CrossRef](#)]
- Giroud, J.P.; Han, J. Design method for geogrid-reinforced unpaved roads (part II): Calibration and verification. *J. Geotech. Geoenviron. Eng.* **2004**, *130*, 787–797. [[CrossRef](#)]
- Ghosh, B.; Fatahi, B.; Khabbaz, H.; Khabbaz, H.; Yin, J.-H. Analytical study for double-layer geosynthetic reinforced load transfer platform on column improved soft soil. *Geotext. Geomembr.* **2017**, *45*, 508–536. [[CrossRef](#)]
- Minghua, Z.; Meng, L.; Rui, Z.; Jun, L. Calculation of load sharing ratio and settlement of bidirectional reinforced composite foundation under embankment loads. *Chin. J. Geotech. Eng.* **2014**, *36*, 2161–2169. [[CrossRef](#)]
- Abusharar, S.W.; Zheng, J.-J.; Chen, B.-G.; Yin, J.-H. A simplified method for analysis of a piled embankment reinforced with geosynthetics. *Geotext. Geomembr.* **2009**, *27*, 39–52. [[CrossRef](#)]
- Yan, Z.; Xiaoyan, C.; Kangyu, W. A Method to Analyze the Settlement of Reinforced Piled Embankment Considering the Three-Dimensional Deformation of Geosynthetic Reinforced Structure. *J. Tianjin Univ. Sci. Technol.* **2019**, *52*, 1227–1234. [[CrossRef](#)]
- Chao, X.; Xiao, L.; Panpan, S. Model tests of tensile membrane effect of geosynthetic-reinforced Piled embankments. *Rock Soil Mech.* **2016**, *37*, 182–1831. [[CrossRef](#)]
- JTG/T D31-02-2013; Technical Guidelines for Design and Construction of Embankment on Soft Ground. China Communications Press: Beijing, China, 2013.
- GB-T 50783-2012; Composite Foundation Technical Specifications. China Planning Press: Beijing, China, 2012.
- BS 8006-1: 2010; Code of Practice for Strengthened/Reinforced Soils and Other Fills. British Standards Institution: London, UK, 2010.
- Nordic Geotechnical Group. *Nordic Guidelines for Reinforced Soils and Fills*; Nordic Geotechnical Group: Stockholm, Sweden, 2004.
- EBGEO 2010; Recommendations for Design and Analysis of Earth Structures Using Geosynthetic Reinforcements. German Geotechnical Society: Berlin, Germany, 2010.
- Girout, R.; Blanc, M.; Thorel, L.; Dias, D. Geosynthetic reinforcement of pile-supported embankments. *Geosynth. Int.* **2018**, *25*, 37–49. [[CrossRef](#)]
- Zhu, X.; Cui, X. Experimental Study on the Effect of Geogrid Reinforcement in Pile-supported Embankment. *J. Hebei Univ. Eng. Nat. Sci. Ed.* **2020**, *37*, 35–40.
- Cui, X.; Zhuang, W.; Xiao, H.; Zhang, J.; Zhang, J. Investigation on soil arching effect in visual model test of pile-supported embankment. *Chin. J. Rock Mech. Eng.* **2020**, *39*, 3150–3158. [[CrossRef](#)]
- Chen, Y.M.; Cao, W.-P.; Chen, R.-P. An experimental investigation of soil arching within basal reinforced and unreinforced piled embankments. *Geotext. Geomembr.* **2008**, *26*, 164–174. [[CrossRef](#)]
- Reshma, B.; Rajagopal, K.; Viswanadham, B.V.S. Centrifuge model studies on the settlement response of geosynthetic piled embankments. *Geosynth. Int.* **2019**, *27*, 170–181. [[CrossRef](#)]
- Briancon, L.; Simon, B. Performance of pile-supported Embankment over soft soil: Full-scale experiment. *J. Geotech. Geoenviron. Eng.* **2012**, *138*, 551–561. [[CrossRef](#)]
- Chen, R.P.; Xu, Z.Z.; Chen, Y.M.; Ling, D.S.; Zhu, B. Field tests on pile-supported embankments over soft ground. *J. Geotech. Geoenviron. Eng.* **2010**, *136*, 777–785. [[CrossRef](#)]
- Cao, W.Z.; Zheng, J.J.; Zhang, J.; Zhang, R.J. Field test of a geogrid-reinforced and floating pile-supported embankment. *Geosynth. Int.* **2016**, *23*, 348–361. [[CrossRef](#)]

21. Zhang, J.; Zheng, J.J.; Lu, Y.E. Evaluation of the new technique of geogrid-reinforced and pile-supported embankment at bridge approach. *J. Bridge Eng.* **2014**, *19*, 06014001. [[CrossRef](#)]
22. Marston, A.; Anderson, A.O. *The Theory of Loads on Pipes in Ditches and Tests of Cement and Clay Drain Tile and Sewer Pipe*; Bulletin No. 31; IA Engineering Experimental Station, Iowa State College: Ames, IA, USA, 1913; p. 181.
23. Hewlett, W.J.; Randolph, M.F. Analysis of piled embankment. *Ground Eng.* **1988**, *21*, 12–18.
24. Chen, Y.; Jia, N.; Chen, R. Soil arch analysis of pile-supported embankments. *China J. Highw. Transp.* **2004**, *17*, 4–9. [[CrossRef](#)]
25. Zaeske, D.; Kempfert, H.G. Calculation and mechanism of unreinforced and reinforced base layers on point and line-shaped support members. *Civ. Eng.* **2002**, *77*, 80–86.